The impact of stratospheric ozone feedbacks on climate sensitivity estimates

Peer J. Nowack[1,2*], N. Luke Abraham[1,3], Peter Braesicke[4] and John A. Pyle[1,3]

[1]Department of Chemistry, Centre for Atmospheric Science,
University of Cambridge, Cambridge, United Kingdom

[2]now at: Grantham Institute, Department of Physics and the Data Science Institute,
Faculty of Natural Sciences, Imperial College London, London, United Kingdom

[3]National Centre for Atmospheric Science, United Kingdom

[4]Karlsruhe Institute of Technology, IMK-ASF, Karlsruhe, Germany

Corresponding author: Peer Nowack (p.nowack@imperial.ac.uk)

Key Points:

- The impacts of different ozone representations in climate sensitivity simulations are assessed with HadGEM3-AO
- We find significant impacts on global warming and other composition-climate feedbacks, such as the stratospheric water vapor feedback
- Our results imply that some ozone implementations in climate sensitivity simulations need to be reconsidered

Abstract

A number of climate modeling studies have shown that differences between typical choices for representing ozone can affect climate change projections. Here, we investigate potential climate impacts of a specific ozone representation used in simulations of the HadGEM model for the Coupled Model Intercomparison Project phase 5. The method considers ozone changes only in the troposphere and lower stratosphere and prescribes stratospheric ozone elsewhere. For a standard climate sensitivity simulation, we find that this method leads to significantly increased global warming and specific patterns of regional surface warming compared with a fully interactive atmospheric chemistry set-up. We explain this mainly by the suppressed part of the stratospheric ozone changes and the associated alteration of the stratospheric water vapor feedback. This combined effect is modulated by simultaneous cirrus cloud changes. We underline the need to understand better how representations of ozone can affect climate modeling results and, in particular, global and regional climate sensitivity estimates.

1 Introduction

Atmospheric ozone is a key absorber of solar radiation and an important greenhouse gas. Consequently, a large sensitivity of surface temperature to ozone changes has been evident for a long time, even in idealized radiative transfer calculations that did not consider many climate feedbacks [e.g. *Lacis et al.*, 1990]. This sensitivity is particularly distinct for ozone changes in the tropical upper troposphere and lower stratosphere (see e.g. Figure 1 in *Riese et al.* [2012]). Here, we explore how considering or (to some extent) neglecting ozone changes under climate change alters the climate sensitivity of a fully interactive atmosphere-ocean coupled climate model. Our work stands in context with a number of recent studies that have confirmed that the representation of ozone in state-of-the-art climate models can affect tropospheric and surface climate change projections [e.g. *Son et al.*, 2008; *Dietmüller et al.*, 2014; *Muthers et al.*, 2014, 2016, *Chiodo and Polvani*, 2016a, 2016b, *Nowack et al.*, 2015, 2017; *Noda et al.*, 2017]. It is further motivated by the apparently strong model- and scenario-dependency of climate impacts associated with changes in ozone. For example, current estimates for the impact of interactive ozone chemistry on global warming projections in a typical climate sensitivity simulation range between none [*Marsh et al.*, 2016] to ~20% difference [*Nowack et al.*, 2015].

Atmospheric chemistry (and thus ozone) has been represented in a variety of ways in climate models, in particular in model intercomparison projects [*Son et al.*, 2008; *Cionni et al.*, 2011; *Taylor et al.*, 2012; *Eyring et al.*, 2013; *Kravitz et al.*, 2013]. For example, only 9 of 46 climate models used to simulate the four Representative Concentration Pathways (RCP) scenarios in the Coupled Model Intercomparison Project 5 (CMIP5) included a fully interactive chemistry scheme both in the troposphere and the stratosphere [*Eyring et al.*, 2013]. In acknowledgement of the importance of ozone, the chemistry-climate community therefore provided a standardized IGAC/SPARC ozone field for RCP simulations to be used in models without atmospheric chemistry component [*Cionni et al.*, 2011]. While this posed an improvement over neglecting ozone changes altogether in many similar CMIP3 simulations [*Son et al.*, 2008], this ozone field was inconsistent with both the actual RCP scenarios and individual model responses. In contrast, there was no organized or unified effort concerning the representation of ozone in typical climate sensitivity simulations in CMIP5, such as those imposing an abrupt quadrupling of atmospheric carbon dioxide (CO_2). As a result, models that lacked the capability to simulate ozone changes on the run had to represent ozone inconsistently, e.g. by neglecting ozone changes, or by using other methods. While it is not well documented how ozone was treated in such cases (with a few

exceptions, e.g. *Jones et al.*, 2011; *Li et al.*, 2013), it is highly likely that the majority of models used unchanged climatologies, or some other form of non-interactive ozone fields in typical climate sensitivity experiments. Consequently, there is a need to understand better how climate sensitivity simulations have been shaped by the representation of ozone in conjunction with other parametric choices. It is almost self-evident that this need for an improved understanding of ozone's role in climate sensitivity simulations extends beyond the CMIP framework.

Here, we investigate one example of potential effects on climate sensitivity projections for a specific ozone representation that was used by the UK Met Office in HadGEM2-ES simulations for the CMIP5 [*Jones et al.*, 2011]. Specifically, we test its effect on the outcome of a standard climate sensitivity simulation in which CO_2 concentrations are abruptly quadrupled. For this, we carry out the same analysis as in a previously published paper [*Nowack et al.*, 2015], where we found that neglecting changes in ozone (also referred to as ozone feedbacks) leads to ~20% increased global warming for the same climate model and experiment.

In HadGEM2-ES, the implementation of this method included an interactive representation of tropospheric and lower stratospheric ozone, i.e. ozone was allowed to respond to the CO_2 forcing in this lower part of the atmosphere. The ozone field was fixed elsewhere, meaning that ozone was not allowed to adapt in the middle-upper stratosphere. In the following, we focus on how this representation of ozone modulates global warming in our model. In addition, we show that it can explain stratospheric water vapor (SVW) results obtained in the corresponding CMIP5 simulation with HadGEM2-ES. Indirectly, this method allows us to test the importance of changes in ozone specifically in the lower part of the atmosphere including the tropical upper troposphere and lower stratosphere (UTLS). At the same time, we explain why it may generally be deceptive to study ozone changes in certain regions in isolation, mainly because ozone concentrations in different parts of the atmosphere are intrinsically coupled.

The method used in HadGEM2-ES should pose an improvement on neglecting ozone changes altogether (as probably done in many climate sensitivity studies), but without detailed study it is impossible to quantify this improvement. We further discuss our results in the context of recent studies on ozone-related effects in climate sensitivity experiments.

2 Methods

2.1. Model

We use the atmosphere-ocean coupled configuration of the Hadley Centre Global Environment Model version 3 (HadGEM3-AO) from the United Kingdom Met Office [*Hewitt et al.*, 2011]. The atmosphere is represented by the Met Office's Unified Model (MetUM) version 7.3 using a regular grid with a horizontal resolution of 3.75° longitude by 2.5° latitude and 60 vertical levels up to a height of ~84 km. The ocean component is the Ocean Parallélisé (OPA) part of the Nucleus for European Modelling of the Ocean (NEMO) model version 3.0 [*Madec*, 2008] coupled to the Los Alamos sea ice model CICE version 4.0 [*Hunke and Lipscomb*, 2008]. The NEMO configuration used here deploys a tripolar, locally anisotropic grid which has 2° resolution in longitude everywhere, but an increased latitudinal resolution in certain regions with up to 0.5° in the tropics.

Atmospheric chemistry is represented by the United Kingdom Chemistry and Aerosols (UKCA) model in an updated version of the detailed stratospheric chemistry configuration [*Morgenstern et al.*, 2009; *Nowack et al.*, 2015, 2016, 2017] which is coupled to the MetUM. A relatively simple tropospheric chemistry scheme that simulates hydrocarbon oxidation is included,

which provides for emissions of three chemical species (NO (surface, lightning), CO (surface), HCHO (surface)). In addition, surface mixing ratios of four further species (N_2O, CH_3Br, H_2, CH_4) are constrained by calculating the effective emission required to maintain their surface mixing ratios, e.g. for nitrous oxide 280 ppbv and for methane 790 ppbv. This keeps their tropospheric mixing ratios approximately constant at preindustrial levels in all simulations. Nitrogen oxide emissions from lightning are parameterized according to *Price and Rind* [1992, 1994]. Photolysis rates are calculated interactively using the Fast-JX photolysis scheme [*Wild et al.*, 2000; *Bian and Prather*, 2002; *Neu et al.*, 2007; *Telford et al.*, 2013]. In total 159 chemical reactions involving 41 chemical species are considered. The chemistry scheme used here is different from the one used for the corresponding HadGEM2-ES simulation in CMIP5, as discussed in section 2.2.

2.2 Simulations

To study the impact of the model representation of ozone on climate sensitivity results, we first carried out a preindustrial control simulation (piControl, 285 ppmv CO_2, label A) and, second, typical climate sensitivity simulations in which atmospheric CO_2 was abruptly quadrupled to four times its preindustrial value (hereafter referred to as 4xCO_2, 1140 ppmv CO_2). Such simulations are standard experiments in model intercomparison projects [*Taylor et al.*, 2012; *Kravitz et al.*, 2013; *Eyring et al.*, 2016]. Each simulation was run for 200 years (for an overview see Table 1).

Type	Label	Representation of Ozone
piControl	A	Interactive in the whole atmosphere
4xCO_2	B	
4xCO_2	D1	Interactive in the troposphere and the lowermost 3 model levels of the stratosphere, prescribed climatology (zonally averaged for D2) from A above
4xCO_2	D2	

Table 1. Overview of the simulations. Two versions (i.e. D1/D2) of the tropopause-matched runs were carried out. The label 1 implies that the chemical fields were overwritten from three model levels above the tropopause upwards by full three-dimensional (latitude, longitude, altitude) monthly-mean climatologies from piControl run A. In D2, the same climatologies were zonally averaged and as such imposed as three-dimensional fields, with almost identical results.

The 4xCO_2 benchmark simulation with fully interactive chemistry is referred to as 'B'. In two further 4xCO_2 simulations, which we here label D1 and D2 in order to conform with a previous paper [*Nowack et al.*, 2017], we emulate the model set-up described by *Jones et al.* [2011] for the abrupt 4xCO_2 experiment carried out with the HadGEM2-ES model for the CMIP5. In D1 and D2, the distribution of the radiatively active species ozone, nitrous oxide and methane was reset to preindustrial levels from three model levels above the continuously changing tropopause [*Hoerling et al.*, 1993] upwards. In other words, ozone was only allowed to change from the surface up to three model levels above the tropopause and was otherwise kept fixed in terms of its mass mixing ratio. The vertical distance between the tropopause and the overwritten

stratospheric levels is between ~3-4 km at all latitudes. This specific methodology used in D1/D2 is referred to as 'tropopause-matching' in the following.

The tropopause-matched model set-up will necessarily include to some degree ozone feedbacks in the tropical upper troposphere and lower stratosphere (UTLS), which were previously identified as a key driver of ozone's impact on climate sensitivity estimates [*Lacis et al.*, 1990; *Forster and Shine*, 1997; *Hansen et al.*, 1997; *Dietmüller et al.*, 2014; *Nowack et al.*, 2015]. It will also prevent an artificial mismatch between ozone and the atmospheric pressure/temperature profiles around the tropopause. This is important due to the steep gradient in ozone mass mixing ratios between the upper troposphere and lower stratosphere, i.e. it prevents high stratospheric ozone levels from being shifted into the troposphere when the latter expands under CO_2 forcing [*Heinemann*, 2009; *Li et al.*, 2013; *Dietmüller et al.*, 2014; *Nowack et al.*, 2015].

The ozone methodology applied in D1/D2 is identical to the set-up of the HadGEM2-ES model for the abrupt 4xCO_2 simulation in CMIP5 and the atmosphere part of HadGEM2-ES is the predecessor model of the atmospheric component of the HadGEM3 model used here. Nevertheless, there are several key differences between our simulations and the HadGEM2-ES implementation. HadGEM2-ES is a low-top model that does not include a full representation of the stratosphere (reaching up to ~40 km altitude, *Collins et al.*, [2011]). In addition, HadGEM2-ES included a somewhat more sophisticated tropospheric chemistry scheme, but no specific stratospheric chemistry, in contrast to the scheme used here. It is impossible to estimate precisely how these and other differences in the model set-up could affect, in relative terms, the results. However, our set-up is sufficient to consider how this alternative representation of ozone feedbacks can affect climate sensitivity, forcing and feedback estimates in a qualitative manner as compared to a fully interactive chemistry configuration.

2.3 Method to estimate climate forcings and feedbacks

In section 3.2, we apply the linear regression methodology suggested by *Gregory et al.* [2004] to diagnose global climate feedbacks and forcings. The method has been shown to capture well the response of models to many types of climate forcing [*Gregory and Webb*, 2008; *Forster et al.*, 2016]. It assumes a linear relationship between the change in global and annual mean radiative imbalance N (Wm^{-2}) at the top of the atmosphere (TOA) and surface temperature anomalies (ΔT_{surf}, in K) relative to a base climate state (typically preindustrial):

$$N = F + \alpha \Delta T_{surf} \qquad (1)$$

where the y-intercept F is the effective forcing (Wm^{-2}) and the slope α is the effective climate feedback parameter ($Wm^{-2}K^{-1}$). Thus, α and F can be obtained by regressing N as a function of time against ΔT_{surf}. α is a characteristic quantity of a given model system, because its magnitude approximates the surface temperature response to a radiative forcing introduced to the system. Here, the positive sign convention is used, meaning that a negative α implies a stable climate system that will eventually attain equilibrium. Any positive/negative change in α implies an additional surface warming/cooling at equilibrium in response to a radiative forcing.

The Gregory method, and more generally energy budget considerations, are often extended by the assumption that the net climate feedback parameter α (and accordingly F) can be approximated by a linear superposition of processes that contribute to the overall climate response to an imposed forcing, i.e.

$$\alpha = \sum_i \alpha_i \qquad (2.1)$$

$$F = \sum_i F_i \quad (2.2)$$

Accordingly, one can decompose α and F into separate radiative components [*Andrews et al.*, 2012]

$$\alpha = \alpha_{CS} + \alpha_{CRE} = \alpha_{CS,LW} + \alpha_{CS,SW} + \alpha_{CRE,LW} + \alpha_{CRE,SW} \quad (3.1)$$

$$F = F_{CS} + F_{CRE} = F_{CS,LW} + F_{CS,SW} + F_{CRE,LW} + F_{CRE,SW} \quad (3.2)$$

providing individual short-wave (SW) and long-wave (LW) components for Clear-Sky (CS) radiative fluxes and the Cloud Radiative Effect (CRE). The CS values refer to idealized radiative calculations in which any cloud effects are left out. The CRE component then represents the difference between the all-sky calculations including clouds and this CS component. In this method, the CRE contains direct effects due to changes in clouds and indirect cloud masking effects, for example due to persistent cloud cover over certain areas of the globe that mask surface albedo changes in the all-sky calculation [*Soden et al.*, 2004, 2008; *Zelinka et al.*, 2013]. The individual α and F components can be obtained by component-wise regressions of the radiative fluxes against ΔT_{surf}.

3 Results

3.1 Surface Warming Response

Figure 1a shows ΔT_{surf} for all runs relative to the average of piControl. Following a sharp increase after the abrupt $4xCO_2$ forcing, surface temperatures for the tropopause-matched runs D1/D2 level off towards a higher equilibrium value than for fully interactive run B. Specifically, the global mean surface warming after 75 years is ~7% larger in D1/D2 than in B, which is about one third of the effect of neglecting ozone feedbacks entirely for the same model [*Nowack et al.*, 2015]. As expected, there is still a remaining temperature trend after 200 years in all $4xCO_2$ runs due to the long oceanic time-scales involved in attaining equilibrium [*Li et al.*, 2013; *Knutti and Rugenstein*, 2015]. Due to the different warming trajectories, the percentage difference decreases slightly over time, approaching ~6.5% towards the end of the 200 years runtime.

Regional surface temperatures also differ significantly between D1/D2 and B and have a specific regional structure (Figures 1b-e). This implies that the stratospheric representation of ozone does not only alter the scaling of the surface temperature response to CO_2 forcing in a globally uniform manner, but has a specific forcing-response pattern and alters regional feedbacks [*Boer and Yu*, 2003a, 2003b; *Shindell and Faluvegi*, 2009; *Voulgarakis and Shindell*, 2010]. A detailed discussion of regional impacts is beyond the scope of this simple global energy budget paper. However, ozone-induced differences in the El Niño Southern Oscillation between the simulations [*Nowack et al.*, 2017], associated changes in atmospheric teleconnections, or a modulating effect of ozone changes on the Atlantic Meridional Overturning Circulation [*Muthers et al.*, 2016] could explain some of these regional responses. The pattern and magnitude of the surface temperature anomalies is mostly very similar for D1 and D2, implying that the surface impacts related to zonal averaging of the ozone climatology are small compared to the ones between B and D1/D2. The existing regional anomalies, for example in the Barents Sea, could be related to the effects of the different zonal structure of the ozone fields used in D1 and D2 on the stratospheric temperature structure and dynamics [*Gabriel et al.*, 2007] and by extension their possible tropospheric impacts. However, a proper analysis would have to take into account a number of other factors, including the state of the ocean and its interaction with sea ice feedbacks.

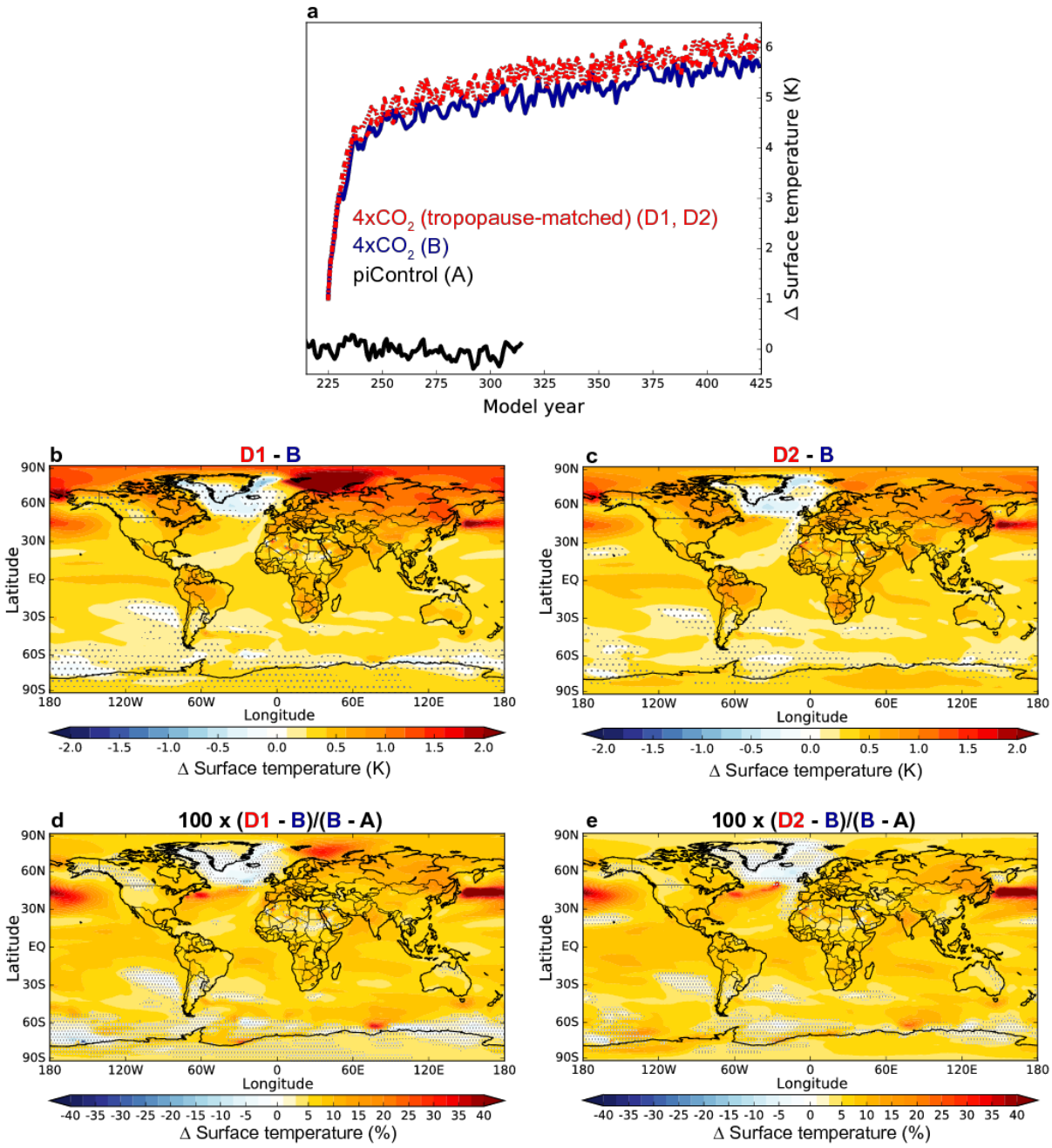

Figure 1. (a) Global, annual mean surface temperature anomalies. The time axis is extended to Figure 1 in *Nowack et al.* [2015]. Red dashed/dotted lines denote runs D1/D2, respectively. (b, c) Regional differences as labeled, averaged over years 275-425 of (a), i.e. years 50-200 after the initialization of the $4xCO_2$ forcing. (d, e) The same regional differences given as percentage changes relative to the warming under $4xCO_2$ for B. The global mean difference is ~7%. Non-significant changes (95% confidence level, two-tailed Student's t-test) are marked by stippling.

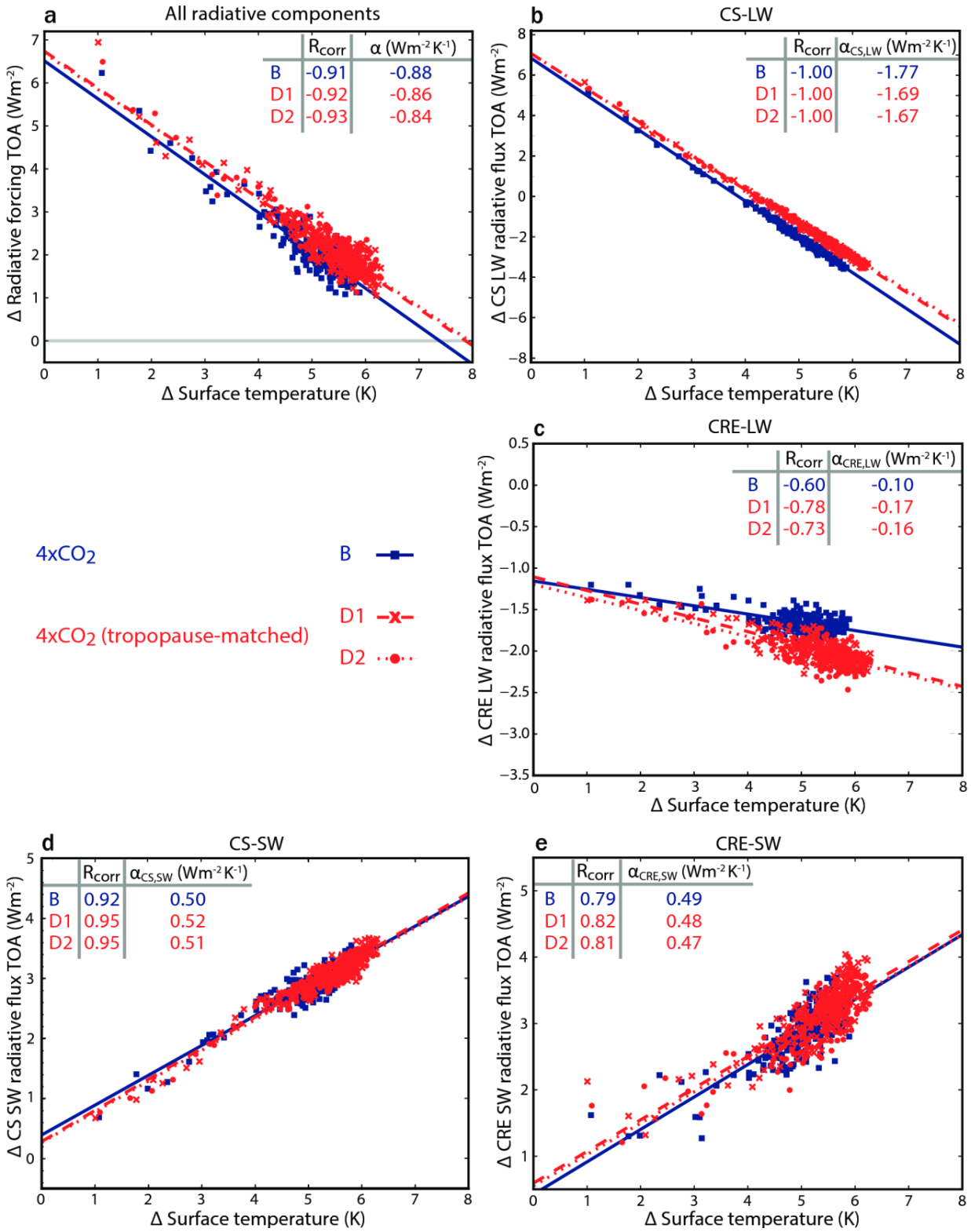

Figure 2. Gregory regressions for all 4xCO_2 simulations as labeled. For (a) the total net TOA radiative flux, (b-e) the four subcomponents. The inset tables give the slopes (i.e. the effective feedback parameters α) and regression coefficients (R_{corr}).

3.2 Global Energy Budget Analysis

To illustrate key differences between the simulations, we carried out the linear regression analysis as described in section 2.3. The results for the all-sky regression and the four individual CS and CRE components are given in Figures 2a-e.

The α feedback parameters of B, D1 and D2 are almost identical (Figure 2a, inset table). The individual CS and CRE components reveal that this is primarily the result of two cancelling factors: the $\alpha_{CS,LW}$ parameters in D1/D2 are less negative (by ~0.1 $Wm^{-2}K^{-1}$, Figure 2b), thus indicating an additional surface warming effect in agreement with the results shown in Figure 1. However, this less negative feedback in D1/D2 is largely compensated by simultaneous, opposite sign $\alpha_{CRE,LW}$ changes (~0.07 $Wm^{-2}K^{-1}$, Figure 2c). The additional surface warming in D1/D2 relative to B would be even more significant without this compensating CRE-LW feedback.

In comparison, changes in the SW components play a minor role (Figures 2d,e). Overall, this gives rise to the very similar, however still slightly less negative total α parameters in D1/D2, consistent with the greater surface warming in these runs. This surplus warming is enhanced by ~0.2 Wm^{-2} more positive effective forcings F in D1/D2 (y-intercepts in Figure 2a). These characterize fast (and actually non-linear; the data deviates from the regression lines towards $\Delta T_{surf} = 0$) adjustments in response to the CO_2 forcing [*Forster et al.*, 2013; *Zelinka et al.*, 2013; *Sherwood et al.*, 2015].

3.3 The Mechanism

The differences in global warming between the simulations can mainly be understood from the representation of ozone and associated SVW and cirrus cloud feedbacks. This argument is equivalent to the mechanism described in *Nowack et al.* [2015] but the absolute and relative magnitude of each contribution differs. As a result, surface temperatures in D1/D2 are closer to B than if ozone feedbacks are neglected altogether (as done in our previous study).

Figures 3a,b show latitude-height cross sections of percentage changes in annual, zonal mean ozone mass mixing ratios under $4xCO_2$ for both the fully interactive and the tropopause-matched runs (here discussed for D2, but with equivalent results for D1). We find characteristic decreases in tropical UTLS ozone within ~30N-30S. This is an ubiquitous feature in chemistry-climate model simulations under increased atmospheric greenhouse gas concentrations that has mainly been explained by an acceleration of the stratospheric Brewer-Dobson circulation [*SPARC*, 2010; *Lin and Fu*, 2013]. Middle-upper stratospheric ozone increases found in the fully interactive run B under CO_2-induced cooling of the stratosphere are also well understood [*Haigh and Pyle*, 1982; *Jonsson et al.*, 2004].

However, the tropopause-matching method fails to capture the full magnitude and spatial extent of the ozone decreases in the tropical UTLS (compare Figures 3a and 3b; for the actual difference between B and D2 see Figure 3c). The proximity to the fixed ozone boundary conditions above tends to level out the ozone decrease below by diffusion. More advective in-mixing of stratospheric ozone into the tropical UTLS via the shallow branch of the Brewer-Dobson circulation will support this effect. The larger mid-to-upper tropospheric ozone increases in D1/D2 than in B are likely the sum of elevated lightning NO_x emissions under greenhouse gas forcing and this greater in-mixing of ozone. In addition, the lack of temperature-driven increases in upper stratospheric ozone in D1/D2 enhances ozone production in the tropical UTLS relative to B due to the reverse self-healing effect of the ozone column [*Pyle*, 1980; *Haigh and Pyle*, 1982; *Meul et al.*, 2014], i.e. changes in ozone formation at different altitudes are anti-correlated as increases in ozone at high altitudes allow less radiation to propagate to lower levels of the

atmosphere, thus reducing ozone production there. Finally, while less important for the climate sensitivity response discussed here, we also find significant differences in the lower stratospheric high latitude response of ozone in D2 compared to B (Figures. 3a-c). The smaller ozone mass mixing ratios found in D2 (and D1) are likely due to the lower ozone concentrations in air transported downwards from the upper stratosphere into this region as part of the upper branch of the Brewer-Dobson circulation [*Plumb*, 2002; *Butchart*, 2014].

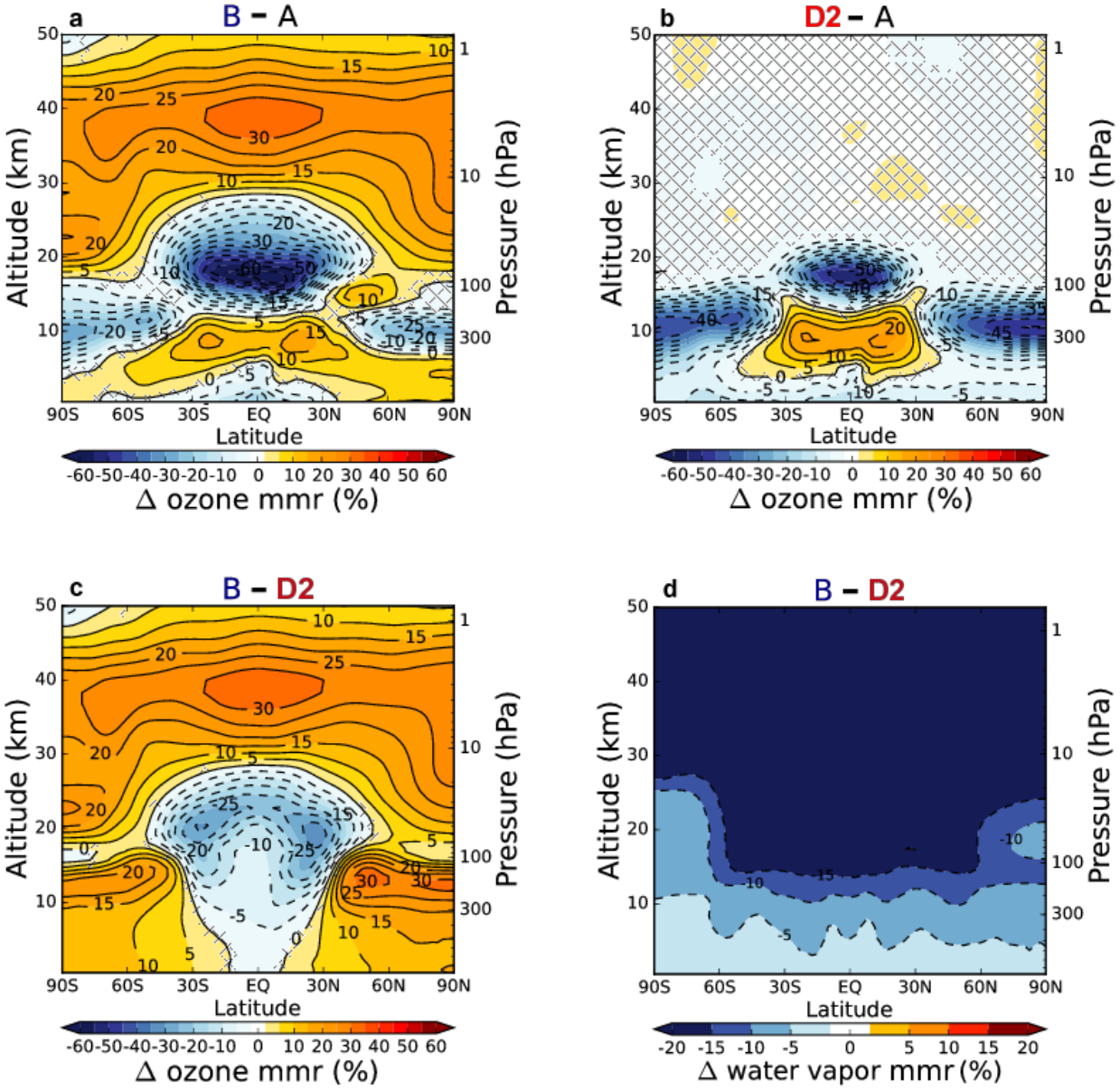

Figure 3. Zonal mean ozone and water vapor percentage differences, as labeled, for years 50-200 after the 4xCO_2 forcing. Non-significant changes at the 95% confidence level using a two-tailed Student's t-test are hatched out. Small artifacts at overwritten altitudes in (b) result from ozone changes between the dynamical and chemistry model time-steps, which occur before the ozone field is reset to preindustrial values. (c) shows the difference between (a) and (b).

Ozone is a key radiative heating agent in the tropical UTLS [*Fueglistaler et al.*, 2009]. Therefore, the decreases in ozone have a pronounced cooling effect there, which accordingly is smaller in D1/D2 than in B (Figures 3c, 4a). This has two important consequences, which mainly explain the less negative $\alpha_{CS\text{-}LW}$ parameters in D1/D2:

1) Ozone is a particularly effective greenhouse gas in the tropical UTLS [*Lacis et al.*, 1990; *Hansen et al.*, 1997; *Stuber et al.*, 2005]. Therefore, the smaller circulation-driven decreases in tropical UTLS ozone in D1/D2 will contribute to the CS-LW differences, compared to B.

2) Higher tropical UTLS temperatures increase the entry rates of water vapor into the stratosphere [*Fueglistaler et al.*, 2005; *Dessler et al.*, 2013], resulting in higher SVW concentrations in D1/D2 than in B (Figure 3d). Since SVW is a greenhouse gas, this amplifies the greenhouse warming effect of the positive ozone anomaly in D1/D2 relative to B [*Stuber et al.*, 2001]. SVW mixing ratios increased by an additional 1.5-2 ppmv in D1/D2 compared to B (absolute increases under $4xCO_2$ are ~1-1.5 ppmv in B and ~3 ppmv in D1/D2; in fact the latter results closely match the HadGEM2-ES results in CMIP5).

Following our argument in *Nowack et al.* [2015], we thus conclude that both changes in tropical UTLS ozone and the associated SVW feedback are the key drivers behind the less negative $\alpha_{CS\text{-}LW}$ parameters (and thus global warming) in D1/D2 than in B.

In D1/D2 the resulting meridional temperature gradient is smaller than in B (Figure 4a). As expected, we find the corresponding weakening of the annual mean mid-latitude stratospheric jet in B (Figure 4b). Within the troposphere, the Hadley cell contracts in B (relative to D2), with stronger zonal winds equatorward, but weaker poleward. This ozone-change induced dynamical response opposes the response to increased CO_2. *Chiodo and Polvani* (2016) discussed a similar phenomenon in the Southern Hemisphere in their sensitivity study, although a direct comparison is difficult, due to slightly different experimental design.

We can also link the feedback differences in the CRE-LW component to a previously described mechanism (see *Nowack et al.* [2015] for details). The temperature effect (Figure 4a) of the underestimated tropical UTLS ozone changes in D1/D2 relative to B leads to reduced formation of upper tropospheric cirrus clouds (Figure 5), which trap LW radiation in the atmosphere [*Kuebbeler et al.*, 2012; *Zelinka et al.*, 2013; *Nowack*, 2015]. Consequently, we find more negative $\alpha_{CRE\text{-}LW}$ parameters in D1/D2 than in B, which reduces the global warming gap between the simulations. In terms of absolute magnitude, this compensating effect almost cancels the CS-LW feedback differences, which gives rise to a much smaller discrepancy in the total feedback parameter α than if the model is run using fixed ozone throughout the entire atmosphere [*Nowack et al.*, 2015]. However, percentage-wise the difference remains almost the same, with the CRE-LW effect being ~60% (70%) of the CS-LW effect for fixed ozone (D1/D2).

Finally, the more positive effective forcing F (larger by ~0.2 Wm^{-2} in the linear approximation) in D1/D2 than in B will contribute to the global warming differences, however, it is mechanistically more difficult to assign. It is the net result of differences in each of the four radiative components (see y-intercepts in Figures 2b-e) that are too small to link to specific processes in a statistically robust manner. However, it is intuitive that fast ozone (and corresponding water vapor, temperature) changes have potential to affect the CS forcings, whereas their impact on absolute temperatures and lapse rates could indirectly affect the CRE forcings. We note that upper stratospheric ozone increases such as the ones suppressed in D1/D2 have mostly been associated with negative SW radiative forcing in studies with idealized ozone perturbations [e.g. *Lacis et al.*, 1990; *Hansen et al.*, 1997]. We find no clear effect of ignoring upper stratospheric ozone changes on the CS-SW effective forcing (Fig. 2d), which might simply be the

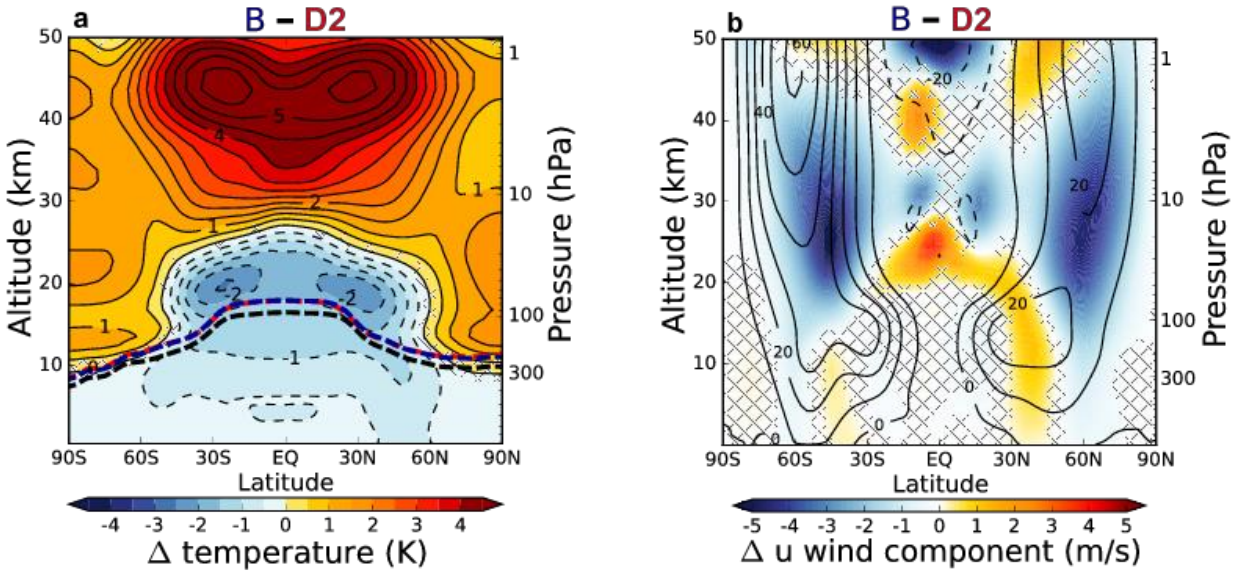

341

342 **Figure 4.** Zonal mean temperature and zonal wind differences, as labeled, for years 50-200 after
343 the 4xCO_2 forcing. In (a), the color scale is constrained to highlight the changes around the
344 tropical tropopause, while the contour lines show the full extent of all changes as 0.5K intervals.
345 The thick dashed lines show the average height of the thermal tropopause for A (black), B (blue)
346 and D2 (red), which is calculated based on the WMO lapse rate definition [*WMO*, 1957]. In (b),
347 contours show the climatology of run B.

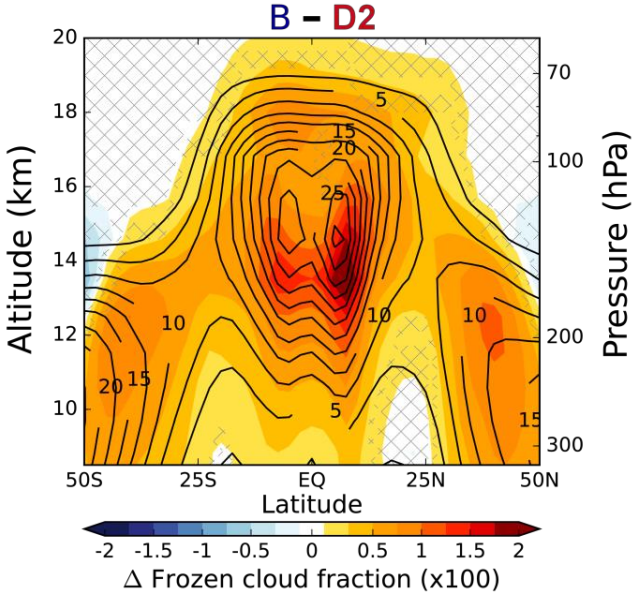

348

349 **Figure 5.** Differences in ice clouds, as labeled, for years 50-200 after the 4xCO_2 forcing. Non-
350 significant changes at the 95% confidence level using a two-tailed Student's t-test are hatched out.
351 The contour lines show the climatology of simulation B.

352 result of its relatively small magnitude as compared to the tropical UTLS LW feedback associated
353 with ozone, in agreement with the SW effects found in other studies [*Dietmüller et al.*, 2014;

Marsh et al., 2016]. The reverse self-healing effect of the ozone column, which was not considered in the idealized perturbation studies, is presumably one reason for the small magnitude. The corresponding opposite sign upper and lower stratospheric changes in ozone are intrinsically coupled and have compensating SW effects.

4 Summary & Conclusions

We have discussed the impact of a specific climate model representation of ozone on the outcome of a standard climate sensitivity simulation. In this representation, ozone changes are only considered in the troposphere and the lowermost three model levels of the stratosphere. Comparing the model response to results obtained when including a fully interactive atmospheric chemistry scheme, we find a larger global warming resulting from (widely even more significant) regional surface temperature changes. These effects are mainly driven by the greenhouse effect of changes in tropical UTLS ozone and the related SVW feedback which, however, is largely balanced by the radiative impact of simultaneous upper tropospheric cirrus cloud changes. We further find that fast adjustments [*Zelinka et al.*, 2013; *Sherwood et al.*, 2015] as a sum over all radiative components (clouds, clear-sky long-wave and short-wave) make a contribution to the larger global warming response. However, these are difficult to assign mechanistically in a statistically significant manner.

Our study has several implications. First, we identify a need to check influences of ozone's representation in climate sensitivity simulations, which are often poorly documented. One example for a non-interactive, but somewhat adaptive ozone representation in a climate sensitivity simulation was given by *Li et al.* [2013]. Using the climate model ECHAM5, they found a very large equilibrium surface warming effect of neglecting ozone changes. They thus decided to shift ozone from the highly sensitive upper troposphere into the upper stratosphere during the simulation, arguing that high levels of stratospheric ozone would otherwise continuously be shifted into the troposphere under CO_2-forced tropospheric expansion. Such physically inconsistent methods will become redundant as more sophisticated atmospheric chemistry components play a key role in the ever increasing complexity of climate models. However, we hope that our study will help to understand past model results better and to motivate further studies in this direction. Ultimately, this could be helpful in tracking progress in climate modeling. For instance, using the same ozone representation, we find SVW increases very similar to those obtained with the predecessor model HadGEM2-ES in CMIP5. Our results thus imply that the use of a fully interactive chemistry scheme could have at least halved the SVW increase found then (from ~3 ppmv to ~1.5 ppmv), which is important for global energy budget considerations as well as atmospheric chemistry [*Shindell*, 2001; *Stenke and Grewe*, 2005; *Stenke et al.*, 2008, 2009; *Solomon et al.*, 2010]. In addition, our study could motivate further research into how model representations of ozone affect regional climate change projections [*Shindell*, 2014; *Marvel et al.*, 2015a, 2015b; *Shindell et al.*, 2015] and key modes of climate variability such as the ENSO [*Chiodo and Polvani*, 2016a; *Nowack et al.*, 2017] rather than just global mean surface temperature change. Finally, our results also bear implications for the efficacy of ozone forcings considering simultaneous cloud feedbacks [*Hansen et al.*, 1997, 2005; *Stuber et al.*, 2005].

In conclusion, we highlight the need to better understand the effects of various model representations of ozone on surface climate change projections, in particular with regard to their impact on results of typical climate sensitivity simulations and the corresponding model-dependency. Among current estimates, the model used here lies at the upper end when it comes to the climate sensitivity impact of neglecting ozone feedbacks entirely, even if the sign of the

response and mechanisms found across most models are robust [*Dietmüller et al.*, 2014; *Muthers et al.*, 2014; *Nowack et al.*, 2015]. Another model showed hardly any net effect on surface temperature [*Marsh et al.*, 2016]. The relatively large sensitivity of our model might imply an also relatively larger effect of the tropopause-height matching implementation on the modeled global warming. However, as implied by Figure 1, even relatively small global mean effects, such as the one found here (6-7%), can correspond to highly significant regional surface temperature changes. We therefore hope that future studies will provide a more complete picture of the impacts of ozone representations on global and regional climate sensitivity estimates.

Acknowledgments

We thank the European Research Council for funding through the ACCI project (project number 267760). The model development was part of the QESM-ESM project supported by the UK Natural Environment Research Council (NERC) under contract numbers RH/H10/19 and R8/H12/124. PJN is supported through an Imperial College Research Fellowship. We acknowledge use of the MONSooN system, a collaborative facility supplied under the Joint Weather and Climate Research Programme, which is a strategic partnership between the UK Met Office and NERC. We used the JASMIN post-processing system [*Lawrence et al.*, 2013] provided through the Centre for Environmental Data Analysis (CEDA). For their roles in producing, coordinating, and making available the HadGEM2-ES CMIP5 model output, we acknowledge the UK Met Office, the World Climate Research Programme's (WCRP) Working Group on Coupled Modelling (WGCM), and the Global Organization for Earth System Science Portals (GO-ESSP). Study-specific data is available through the first author or CEDA (url: http://catalogue.ceda.ac.uk/uuid/3d23afc9bb024c558058749faae4cf2d).

References

Andrews, T., J. M. Gregory, M. J. Webb, and K. E. Taylor (2012), Forcing, feedbacks and climate sensitivity in CMIP5 coupled atmosphere-ocean climate models, *Geophys. Res. Lett.*, *39*, L09712, doi:10.1029/2012GL051607.

Bian, H., and M. J. Prather (2002), Fast-J2: Accurate simulation of stratospheric photolysis in global chemical models, *J. Atmos. Chem.*, *41*(3), 281–296, doi:10.1023/A:1014980619462.

Boer, G. J., and B. Yu (2003a), Climate sensitivity and response, *Clim. Dyn.*, *20*, 415–429, doi:10.1007/s00382-002-0283-3.

Boer, G. J., and B. Yu (2003b), Dynamical aspects of climate sensitivity, *Geophys. Res. Lett.*, *30*(3), 1135, doi:10.1029/2002GL016549.

Butchart, N. (2014), Reviews of Geophysics The Brewer-Dobson circulation, *Rev. Geophys.*, *52*, 157–184, doi:10.1002/2013RG000448.One.

Chiodo, G., and L. M. Polvani (2016a), Reduced Southern Hemispheric circulation response to quadrupled CO2 due to stratospheric ozone feedback, *Geophys. Res. Lett.*, *43*, 1–10, doi:10.1002/2016GL071011.

Chiodo, G., and L. M. Polvani (2016b), Reduction of climate sensitivity to solar forcing due to stratospheric ozone feedback, *J. Clim.*, *29*, 4651–4663, doi:10.1175/JCLI-D-15-0721.1.

Cionni, I., V. Eyring, J. F. Lamarque, W. J. Randel, D. S. Stevenson, F. Wu, G. E. Bodeker, T. G. Shepherd, D. T. Shindell, and D. W. Waugh (2011), Ozone database in support of CMIP5 simulations: Results and corresponding radiative forcing, *Atmos. Chem. Phys.*, *11*(21), 11267–11292, doi:10.5194/acp-11-11267-2011.

Collins, W. J. et al. (2011), Development and evaluation of an Earth-System model – HadGEM2,

444 *Geosci. Model Dev.*, *4*(4), 1051–1075, doi:10.5194/gmd-4-1051-2011.
445 Dessler, A. E., M. R. Schoeberl, T. Wang, S. M. Davis, and K. H. Rosenlof (2013), Stratospheric
446 water vapor feedback., *Proc. Natl. Acad. Sci. U. S. A.*, *110*(45), 18087–91,
447 doi:10.1073/pnas.1310344110.
448 Dietmüller, S., M. Ponater, and R. Sausen (2014), Interactive ozone induces a negative feedback in
449 CO2-driven climate change simulations, *J. Geophys. Res. Atmos.*, *119*, 1796–1805,
450 doi:10.1002/2013JD020575.
451 Eyring, V. et al. (2013), Long-term ozone changes and associated climate impacts in CMIP5
452 simulations, *J. Geophys. Res. Atmos.*, *118*, 5029–5060, doi:10.1002/jgrd.50316.
453 Eyring, V., S. Bony, G. A. Meehl, C. A. Senior, B. Stevens, R. J. Stouffer, and K. E. Taylor
454 (2016), Overview of the Coupled Model Intercomparison Project Phase 6 (CMIP6)
455 experimental design and organization, *Geosci. Model Dev.*, *9*(5), 1937–1958,
456 doi:10.5194/gmd-9-1937-2016.
457 Forster, P. M., T. Andrews, P. Good, J. M. Gregory, L. S. Jackson, and M. Zelinka (2013),
458 Evaluating adjusted forcing and model spread for historical and future scenarios in the
459 CMIP5 generation of climate models, *J. Geophys. Res. Atmos.*, *118*(3), 1139–1150,
460 doi:10.1002/jgrd.50174.
461 Forster, P. M., T. Richardson, A. C. Maycock, C. J. Smith, B. H. Samset, G. Myhre, T. Andrews,
462 R. Pincus, and M. Schulz (2016), Journal of Geophysical Research : Atmospheres, *J.*
463 *Geophys. Res. Atmos.*, *121*, 12460–12475, doi:10.1002/2016JD025320.
464 Forster, P. M. D. E., and K. P. Shine (1997), Radiative forcing and temperature trends from
465 stratospheric ozone changes, *J. Geophys. Res.*, *102*(D9), 10841–10855.
466 Fueglistaler, S., M. Bonazzola, P. H. Haynes, and T. Peter (2005), Stratospheric water vapor
467 predicted from the Lagrangian temperature history of air entering the stratosphere in the
468 tropics, *J. Geophys. Res. Atmos.*, *110*, D08107, doi:10.1029/2004JD005516.
469 Fueglistaler, S., A. E. Dessler, T. J. Dunkerton, I. Folkins, Q. Fu, and P. W. Mote (2009), Tropical
470 tropopause layer, *Rev. Geophys.*, *47*, RG1004.
471 Gabriel, A., D. Peters, I. Kirchner, and H. F. Graf (2007), Effect of zonally asymmetric ozone on
472 stratospheric temperature and planetary wave propogation, *Geophys. Res. Lett.*, *34*(6),
473 doi:10.1029/2006GL028998.
474 Gregory, J. M., and M. Webb (2008), Tropospheric adjustment induces a cloud component in CO2
475 forcing, *J. Clim.*, *21*(1), 58–71, doi:10.1175/2007JCLI1834.1.
476 Gregory, J. M., W. J. Ingram, M. A. Palmer, G. S. Jones, P. A. Stott, R. B. Thorpe, J. A. Lowe, T.
477 C. Johns, and K. D. Williams (2004), A new method for diagnosing radiative forcing and
478 climate sensitivity, *Geophys. Res. Lett.*, *31*(October 2003), L03205,
479 doi:10.1029/2003GL018747.
480 Haigh, J. D., and J. A. Pyle (1982), Ozone perturbation experiments in a two-dimensional
481 circulation model, *Quart. J. R. Met. Soc.*, *108*, 551–574.
482 Hansen, J., M. Sato, and R. Ruedy (1997), Radiative forcing and climate response, *J. Geophys.*
483 *Res. Atmos.*, *102*(D6), 6831–6864, doi:10.1029/96JD03436.
484 Hansen, J. et al. (2005), Efficacy of climate forcings, *J. Geophys. Res.*, *110*(D18), D18104,
485 doi:10.1029/2005JD005776.
486 Heinemann, M. (2009), Warm and sensitive Paleocene-Eocene climate, Max Planck Institute for
487 Meteorology, Hamburg, Germany.
488 Hewitt, H. T., D. Copsey, I. D. Culverwell, C. M. Harris, R. S. R. Hill, A. B. Keen, A. J. McLaren,
489 and E. C. Hunke (2011), Design and implementation of the infrastructure of HadGEM3: The
490 next-generation Met Office climate modelling system, *Geosci. Model Dev.*, *4*(2), 223–253,

491 doi:10.5194/gmd-4-223-2011.
492 Hoerling, M. P., T. K. Schaack, and A. J. Lenzen (1993), A global analysis of stratospheric-
493 tropospheric exchange during northern winter, *Mon. Weather Rev.*, *21*(1), 162–172,
494 doi:10.1175/1520-0493(1993)121<0162:AGAOSE>2.0.CO;2.
495 Hunke, E. C., and W. H. Lipscomb (2008), the Los Alamos sea ice model documentation and
496 software user's manual, Version 4.0, LA-CC-06-012, Los Alamos National Laboratory,
497 N.M.,
498 Jones, C. D. et al. (2011), The HadGEM2-ES implementation of CMIP5 centennial simulations,
499 *Geosci. Model Dev.*, *4*, 543–570, doi:10.5194/gmdd-4-689-2011.
500 Jonsson, A. I., J. de Grandpré, V. I. Fomichev, J. C. McConnell, and S. R. Beagley (2004),
501 Doubled CO2-induced cooling in the middle atmosphere: Photochemical analysis of the
502 ozone radiative feedback, *J. Geophys. Res.*, *109*, D24103, doi:10.1029/2004JD005093.
503 Knutti, R., and M. A. A. Rugenstein (2015), Feedbacks , climate sensitivity and the limits of linear
504 models, *Philos. Trans. R. Soc. A*, *373*, 20150146.
505 Kravitz, B., A. Robock, P. M. Forster, J. M. Haywood, M. G. Lawrence, and H. Schmidt (2013),
506 An overview of the Geoengineering Model Intercomparison Project (GeoMIP), *J. Geophys.*
507 *Res. Atmos.*, *118*(23), 13103–13107, doi:10.1002/2013JD020569.
508 Kuebbeler, M., U. Lohmann, and J. Feichter (2012), Effects of stratospheric sulfate aerosol geo-
509 engineering on cirrus clouds, *Geophys. Res. Lett.*, *39*(23), L23803,
510 doi:10.1029/2012GL053797.
511 Lacis, A. A., D. J. Wuebbles, and J. A. Logan (1990), Radiative forcing of climate by changes in
512 the vertical distribution of ozone, *J. Geophys. Res.*, *95*(D7), 9971–9981,
513 doi:10.1029/JD095iD07p09971.
514 Lawrence, B. N., V. L. Bennett, J. Churchill, M. Juckes, P. Kershaw, S. Pascoe, S. Pepler, M.
515 Pritchard, and A. Stephens (2013), Storing and manipulating environmental big data with
516 JASMIN, *Proc. - 2013 IEEE Int. Conf. Big Data, Big Data 2013*, 68–75,
517 doi:10.1109/BigData.2013.6691556.
518 Li, C., J.-S. von Storch, and J. Marotzke (2013), Deep-ocean heat uptake and equilibrium climate
519 response, *Clim. Dyn.*, *40*(5–6), 1071–1086, doi:10.1007/s00382-012-1350-z.
520 Lin, P., and Q. Fu (2013), Changes in various branches of the Brewer-Dobson circulation from an
521 ensemble of chemistry climate models, *J. Geophys. Res. Atmos.*, *118*(1), 73–84,
522 doi:10.1029/2012JD018813.
523 Madec, G. (2008), *NEMO ocean engine, Note du Pole de modelisation, Institut Pierre-Simon*
524 *Laplace (IPSL)*, 27th ed., France.
525 Marsh, D. R., A. J. Conley, and L. M. Polvani (2016), Stratospheric ozone chemistry feedbacks
526 are not critical for the determination of climate sensitivity in CESM1 (WACCM), *Geophys.*
527 *Res. Lett.*, *43*, 3928–3934, doi:10.1002/2016GL068344.
528 Marvel, K., G. A. Schmidt, D. Shindell, C. Bonfils, A. N. LeGrande, L. Nazarenko, and K.
529 Tsigaridis (2015a), Do responses to different anthropogenic forcings add linearly in climate
530 models?, *Environ. Res. Lett.*, *10*, 104010, doi:10.1088/1748-9326/10/10/104010.
531 Marvel, K., G. A. Schmidt, R. L. Miller, and L. S. Nazarenko (2015b), Implications for climate
532 sensitivity from the response to individual forcings, *Nat. Clim. Chang.*, *6*, 386–389,
533 doi:10.1038/nclimate2888.
534 Meul, S., U. Langematz, S. Oberländer, H. Garny, and P. Jöckel (2014), Chemical contribution to
535 future tropical ozone change in the lower stratosphere, *Atmos. Chem. Phys.*, *14*(6), 2959–
536 2971, doi:10.5194/acp-14-2959-2014.
537 Morgenstern, O., P. Braesicke, F. M. O'Connor, A. C. Bushell, C. E. Johnson, S. M. Osprey, and

538 J. A. Pyle (2009), Evaluation of the new UKCA climate-composition model – Part 1: The
539 stratosphere, *Geosci. Model Dev.*, *2*(1), 43–57, doi:10.5194/gmd-2-43-2009.
540 Muthers, S. et al. (2014), The coupled atmosphere–chemistry–ocean model SOCOL-MPIOM,
541 *Geosci. Model Dev.*, *7*(5), 2157–2179, doi:10.5194/gmd-7-2157-2014.
542 Muthers, S., C. C. Raible, E. Rozanov, and T. F. Stocker (2016), Response of the AMOC to
543 reduced solar radiation - The modulating role of atmospheric chemistry, *Earth Syst. Dyn.*,
544 *7*(4), 877–892, doi:10.5194/esd-7-877-2016.
545 Neu, J. L., M. J. Prather, and J. E. Penner (2007), Global atmospheric chemistry: Integrating over
546 fractional cloud cover, *J. Geophys. Res. Atmos.*, *112*, D11306, doi:10.1029/2006JD008007.
547 Noda, S., K. Kodera, Y. Adachi, M. Deushi, A. Kitoh, R. Mizuta, S. Murakami, K. Yoshida, and
548 S. Yoden (2017), Impact of interactive chemistry of stratospheric ozone on southern
549 hemisphere paleoclimate simulation, *J. Geophys. Res. Atmos.*, *122*, 878–895,
550 doi:10.1002/2016JD025508.
551 Nowack, P. J. (2015), Cirrus and the Earth system, *Weather*, *70*(11), 330, doi:10.1002/wea.2550.
552 Nowack, P. J., N. Luke Abraham, A. C. Maycock, P. Braesicke, J. M. Gregory, M. M. Joshi, A.
553 Osprey, and J. A. Pyle (2015), A large ozone-circulation feedback and its implications for
554 global warming assessments, *Nat. Clim. Chang.*, *5*(1), 41–45, doi:10.1038/nclimate2451.
555 Nowack, P. J., N. L. Abraham, P. Braesicke, and J. A. Pyle (2016), Stratospheric ozone changes
556 under solar geoengineering: implications for UV exposure and air quality, *Atmos. Chem.*
557 *Phys.*, *16*, 4191–4203, doi:10.5194/acpd-15-31973-2015.
558 Nowack, P. J., P. Braesicke, N. L. Abraham, and J. A. Pyle (2017), On the role of ozone feedback
559 in the ENSO amplitude response under global warming, *Geophys. Res. Lett.*, *44*,
560 doi:10.1002/2016GL072418.
561 Plumb, R. A. (2002), Stratospheric Transport, *J. Meteorol. Soc. Japan*, *80*, 793–809,
562 doi:10.2151/jmsj.80.793.
563 Price, C., and D. Rind (1992), A simple lightning parameterization for calculating global lightning
564 distributions, *J. Geophys. Res. Atmos.*, *97*(D9), 9919–9933, doi:10.1029/92JD00719.
565 Price, C., and D. Rind (1994), Modeling Global Lightning Distributions in a General Circulation
566 Model, *Mon. Weather Rev.*, *122*(8), 1930–1939, doi:10.1175/1520-
567 0493(1994)122<1930:MGLDIA>2.0.CO;2.
568 Pyle, J. A. (1980), A calculation of the possible depletion of ozone by chlorofluorocarbons using a
569 two-dimensional model, *Pure Appl. Geophys. PAGEOPH*, *118*, 355–377.
570 Riese, M., F. Ploeger, A. Rap, B. Vogel, P. Konopka, M. Dameris, and P. Forster (2012), Impact
571 of uncertainties in atmospheric mixing on simulated UTLS composition and related radiative
572 effects, *J. Geophys. Res.*, *117*(D16), D16305, doi:10.1029/2012JD017751.
573 Sherwood, S. C., S. Bony, O. Boucher, C. Bretherton, P. M. Forster, J. M. Gregory, and B.
574 Stevens (2015), Adjustments in the forcing-feedback framework for understanding climate
575 change, *Bull. Am. Meteorol. Soc.*, *96*(2), 217–228, doi:10.1175/BAMS-D-13-00167.1.
576 Shindell, D., and G. Faluvegi (2009), Climate response to regional radiative forcing during the
577 twentieth century, *Nat. Geosci.*, *2*(4), 294–300, doi:10.1038/ngeo473.
578 Shindell, D. T. (2001), Climate and ozone response to increased stratospheric water vapor,
579 *Geophys. Res. Lett.*, *28*(8), 1551–1554, doi:10.1029/1999GL011197.
580 Shindell, D. T. (2014), Inhomogeneous forcing and transient climate sensitivity, *Nat. Clim.*
581 *Chang.*, *4*, 274–277, doi:10.1038/NCLIMATE2136.
582 Shindell, D. T., G. Faluvegi, L. Rotstayn, and G. Milly (2015), Spatial patterns of radiative forcing
583 and surface temperature response, *J. Geophys. Res. Atmos.*, n/a-n/a,
584 doi:10.1002/2014JD022752.

585 Soden, B. J., A. J. Broccoli, and R. S. Hemler (2004), On the use of cloud forcing to estimate
586 cloud feedback, *J. Clim.*, *17*(19), 3661–3665, doi:10.1175/1520-
587 0442(2004)017<3661:OTUOCF>2.0.CO;2.
588 Soden, B. J., I. M. Held, R. C. Colman, K. M. Shell, J. T. Kiehl, and C. A. Shields (2008),
589 Quantifying climate feedbacks using radiative kernels, *J. Clim.*, *21*(14), 3504–3520,
590 doi:10.1175/2007JCLI2110.1.
591 Solomon, S., K. H. Rosenlof, R. W. Portmann, J. S. Daniel, S. M. Davis, T. J. Sanford, and G.-K.
592 Plattner (2010), Contributions of stratospheric water vapor to decadal changes in the rate of
593 global warming., *Science (80-.).*, *327*(5970), 1219–1223, doi:10.1126/science.1182488.
594 Son, S.-W., L. M. Polvani, D. W. Waugh, H. Akiyoshi, R. Garcia, D. Kinnison, S. Pawson, E.
595 Rozanov, T. G. Shepherd, and K. Shibata (2008), The impact of stratospheric ozone recovery
596 on the Southern Hemisphere westerly jet., *Science (80-.).*, *320*(5882), 1486–1489,
597 doi:10.1126/science.1155939.
598 SPARC (2010), *SPARC CCMVal Report on the Evaluation of Chemistry-Climate Models*, edited
599 by V. Eyring, T. G. Shepherd, and D. W. Waugh, SPARC Report No. 5, WCRP-132,
600 WMO/TD-No. 1526.
601 Stenke, A., and V. Grewe (2005), Simulation of stratospheric water vapor trends: impact on
602 stratospheric ozone chemistry, *Atmos. Chem. Phys.*, *5*(5), 1257–1272, doi:10.5194/acp-5-
603 1257-2005.
604 Stenke, A., V. Grewe, and M. Ponater (2008), Lagrangian transport of water vapor and cloud
605 water in the ECHAM4 GCM and its impact on the cold bias, *Clim. Dyn.*, *31*, 491–506,
606 doi:10.1007/s00382-007-0347-5.
607 Stenke, A., M. Dameris, V. Grewe, and H. Garny (2009), Implications of Lagrangian transport for
608 simulations with a coupled chemistry-climate model, *Atmos. Chem. Phys.*, *9*, 5489–5504.
609 Stuber, N., M. Ponater, and R. Sausen (2001), Is the climate sensitivity to ozone perturbations
610 enhanced by stratospheric water vapor feedback?, *Geophys. Res. Lett.*, *28*(15), 2887–2890,
611 doi:10.1029/2001GL013000.
612 Stuber, N., M. Ponater, and R. Sausen (2005), Why radiative forcing might fail as a predictor of
613 climate change, *Clim. Dyn.*, *24*(5), 497–510, doi:10.1007/s00382-004-0497-7.
614 Taylor, K. E., R. J. Stouffer, and G. A. Meehl (2012), An overview of CMIP5 and the experiment
615 design, *Bull. Am. Meteorol. Soc.*, *93*(4), 485–498, doi:10.1175/BAMS-D-11-00094.1.
616 Telford, P. J., N. L. Abraham, A. T. Archibald, P. Braesicke, M. Dalvi, O. Morgenstern, F. M.
617 O'Connor, N. A. D. Richards, and J. A. Pyle (2013), Implementation of the Fast-JX
618 Photolysis scheme (v6.4) into the UKCA component of the MetUM chemistry-climate model
619 (v7.3), *Geosci. Model Dev.*, *6*(1), 161–177, doi:10.5194/gmd-6-161-2013.
620 Voulgarakis, A., and D. T. Shindell (2010), Constraining the Sensitivity of Regional Climate with
621 the Use of Historical Observations, *J. Clim.*, *23*, 6068–6073, doi:10.1175/2010JCLI3623.1.
622 Wild, O., X. Zhu, and M. J. Prather (2000), Fast-J: Accurate simulation of in- and below-cloud
623 photolysis in tropospheric chemical models, *J. Atmos. Chem.*, *37*(3), 245–282,
624 doi:10.1023/A:1006415919030.
625 WMO (1957), Meteorology - a three dimensional science: second session of the Commission for
626 Aerology, in *WMO Bull 4*, pp. 134–138.
627 Zelinka, M. D., S. A. Klein, K. E. Taylor, T. Andrews, M. J. Webb, J. M. Gregory, and P. M.
628 Forster (2013), Contributions of different cloud types to feedbacks and rapid adjustments in
629 CMIP5, *J. Clim.*, *26*(14), 5007–5027, doi:10.1175/JCLI-D-12-00555.1.
630